Novel Features to Capture Temporal Variations of Rhythmic Limb Movement to Distinguish Convulsive Epileptic and Psychogenic Non-epileptic Seizures

Shitanshu Kusmakar *Student Member, IEEE,* Chandan K. Karmakar *Member, IEEE,* Bernard Yan, Patrick Kwan, Terence J.O'Brien, Ramanathan Muthuganapathy, and Marimuthu Palaniswami, *Fellow, IEEE*

***Abstract*—Objective: Diagnosis of convulsive psychogenic non-epileptic seizures (PNES) pose a challenge due to their clinical similarities with generalized tonic-clonic seizures. The delay in correct diagnosis of PNES increases the vulnerability to side-effects of anti epileptic drugs and imposes physical, social, and economic burden on patients with PNES. Definite diagnosis of PNES require long term video-electroencephalography monitoring (VEM). However, VEM requires significant system resources and thus, arises the need for alternative methods for PNES diagnosis. In this study, we aim to investigate the potential of Poincaré derived temporal variations in rhythmic limb movement recorded using a wrist-worn accelerometer based device for differentiating convulsive ES and PNES.**

Methods: The temporal variations in the accelerometer traces corresponding to 39 **generalized tonic-clonic seizures (GTCS) and** 44 **convulsive PNES events are obtained using Poincaré maps. Poincaré maps are geometrical representation of a time series signal, when plotted in Cartesian plane. The two proposed indexes: tonic index (*TI*) and dispersion decay index (*DDI*) are calculated to quantify the temporal variations derived using Poincaré maps.**

Key Findings: The *TI* captures the presence of a tonic phase in an event. Whereas, the *DDI* captures the subsiding behavior of an event. *TI* and *DDI* of GTCS events was higher in comparison to convulsive PNES events ($p < 0.001$). A maximum AUC (area under ROC curve) of 0.96 **was obtained for GTCS and PNES differentiation using *TI* alone. A linear discriminant classifier build using a combination of *TI* and *DDI* of all Poincaré derived descriptors could correctly differentiate** 42 **(sensitivity:** 95.45%**) of** 44 **PNES events and** 36 **(specificity:** 92.30%**) of** 39 **GTCS events. A blinded review of the Poincaré derived temporal variations in rhythmic limb movement during seizures could correctly differentiate** 26 **(sensitivity:** 70.27%**) of** 44 **PNES events and** 33 **(specificity:** 86.84%**) of** 39 **GTCS events. In comparison to the proposed method, the coefficient of variation (COV) of limb movement frequency in time windows of** 2.56*s* **resulted in an AUC value of** 0.78**.**

Significance: Temporal variations in rhythmic limb movement can be used to distinguish generalized tonic-clonic seizures (GTCS) from convulsive psychogenic non-epileptic seizures (PNES). Thus, enabling real-time monitoring and differential diagnosis of convulsive PNES, using a wrist-worn accelerometer based biosensor.

***Index Terms*—Temporal variability,** Poincaré **plot, generalized tonic-clonic seizures (GTCS), psychogenic non-epileptic seizures (PNES), accelerometry.**

S. Kusmakar and M. Palaniswami are with the Department of Electrical and Electronic Engineering, The University of Melbourne, Vic - 3052, Australia. Email: skusmakar@student.unimelb.edu.au; palani@unimelb.edu.au

C. K. Karmakar is with the Department of Electrical and Electronic Engineering, The University of Melbourne, Vic - 3052, Australia and also with Deakin University Geelong, Vic - 3125, Australia, Email: karmakar@unimelb.edu.au

R. Muthuganapathy is with the Department of Engineering Design, Indian Institute of Technology Madras, India. Email: mraman@iitm.ac.in

B. Yan, Patrick kwan, and T. O'Brien are with the Melbourne Brain Centre, Royal Melbourne Hospital, Dept. of Medicine, The University of Melbourne, VIC - 3052, Australia. Email: Bernard.Yan@mh.org.au, obrientj@unimelb.edu.au

I. Introduction

Psychogenic non-epileptic seizures (PNES) can be characterized as sporadic paroxysmal events that are accompanied by a change in state of consciousness or behaviour without any epileptiform activity in the brain [1]. There is no known pathophysiologicaly defined pathway for PNES however, PNES events are found to have a causal association to sporadic attacks resulting from autonomic malfunction often linked to major psychoscoial distress [2]. PNES are involuntary, and can be associated with random movements, sensory, and mental manifestations similar to generalized epileptic seizures [3].

Although many pathophysiological features such as: postictal serum prolactin, postictal confusion, eye-widening, seizure duration, and stertorous breathing among others, have been more or less associated with PNES, the sensitivity and specificity of these features is insufficient to establish a definitive diagnosis of PNES [4]. There are no consistent features that can be more or less associated with PNES thus, the definitive diagnosis of PNES remain challenging [5]. Moreover, patients with PNES are often diagnosed with concurrent epileptic seizures [6]. This indicates that out-patient diagnosis of PNES is difficult and PNES is often misdiagnosed as epileptic seizure [7]. Mismanagement and delayed diagnosis of PNES increases the risk of morbidity and mortality due to intubation from prolonged seizures [8]. In addition, misdiagnoses detracts from treating the associated psychopathology, and exposes the patient to adverse side-effects of anti-epileptic drugs (AED) [9]. A mean delay of 5.2 years was reported until the correct diagnosis of PNES [1]. This indicates the short-comings and unsatisfactory nature of current diagnostic procedures [1].

The definitive diagnosis of PNES requires long-term video-electroencephalography monitoring (VEM). However, VEM is a highly resource intensive procedure incuring significant

healthcare cost [10]. Moreover, the limited monitoring period and the hospital environment may potentially impede the quality and the number of captured seizure activity [6]. In addition, VEM is also susceptible to artifacts in electroencephalography (EEG) recording due to movement or suboptimal placement of electrodes, noise in EEG recording can render the study non-diagnostic [6]. Moreover, the availability of VEM is limited to super-specialty and tertiary care hospitals and is not available in countries of low socio economic status [10]. In comparison to patients with delayed diagnosis of PNES, individuals with timely intervention and correct diagnosis of PNES are shown to have a better treatment outcome [11].

The widespread use of VEM for diagnosis of PNES suggests that visual cues embed important parameters for differentiation of PNES. This indicates a possibility of differential diagnosis of PNES outside the hospital environment. Generalized tonic-clonic seizure is the differential diagnosis of PNES [4]. Accelerometers have been shown as an effective tool for detection of convulsive seizures especially, GTCS [12]. In our previous work [13] [14], we showed that accelerometers can be reliably used for detection of convulsive PNES events. However, differential diagnosis of convulsive PNES requires identification of unique features that can distinguish epileptic and non-epileptic motor manifestation. In our previous work [15], we had shown that rhythmic movement activity captured using wrist-worn accelerometer sensors can differentiate GTCS and PNES events. However, the approach was based on short time Fourier transform (STFT) analysis. In context of a wearable device, fast Fourier transform (FFT) algorithm is computationally expensive. Moreover, STFT analysis gives a single frequency based index for differentiation. Therefore, in this work we intend to investigate alternate methods, such that: (1) GTCS and convulsive PNES events can be differentiated using time-domain features; and (2) multiple time domain parameters can be extracted for differentiation of GTCS and convulsive PNES. In this work, we propose new features based on extracting temporal variations in rhythmic limb movement during an event using Poincaré maps [16]. Poincaré maps have been used extensively in analysis of biomedical signals [17]. In addition, Poincaré map is a time-domain technique, and time-domain methods are shown to be better than frequency domain approaches in analysis of non-stationary time-varying signals like the movement of limbs during a seizure [18].

An ambulatory monitoring device for differential diagnosis of convulsive PNES can potentially reduce the diagnostic delay in PNES thus, translating into a better treatment outcome. Therefore, we envision to develop an easy to wear accelerometer based ambulatory monitoring device that can differentiate convulsive PNES and GTCS based on the rhythmic movement activity of limbs during an event. Approaches based on surface electromyography (sEMG) [19], and electrocardiography (ECG) derived heart-rate variability (HRV) [20] have been investigated for differential diagnosis of PNES and GTCS. The sEMG based approach differentiated GTCS and PNES with 100% sensitivity while, the HRV showed a sensitivity of 73%. However, both sEMG and HRV may not be suitable to ambulatory monitoring owing to the continuous use of electrodes and the susceptibility to movement artifacts [21].

To the best of our knowledge, no study based on quantification of temporal dynamics of limb movement during GTCS and convulsive PNES has yet been published. This study delves into investigation of: (1) quantitative accelerometry features that can differentiate GTCS and convulsive PNES; and (2) establish the relevance and clinical utility of a wrist-worn accelerometer based device. If the proposed approach shows a good accuracy in differential diagnosis of GTCS and convulsive PNES, it will have the potential to be utilized as a semi or completely automated tool for diagnosis of convulsive PNES without VEM. The proposed approach can potentially lead to early and low-cost diagnosis of convulsive PNES.

II. Motivation

A GTCS event has a clearly defined seizure semiology as seen on video-EEG [22]. Majority of GTCS events involves following phases: onset of generalization (involving head/body movement or vocalization), pretonic clonic (irregular and asymmetric jerking preceding tonic phase), tonic (sustained contraction of muscles), tremulousness (decrease in muscle tone and beginning of clonic jerking), and clonic phase (clonic jerking) [22]. Whereas, we observed that there was no clear distinction between phases during convulsive PNES events and majority of events were stereotypical of clonus activity. Moreover, not all GTCS events included all phases or had a clear distinction between phases however, all GTCS events can be characterized using a combination of the aforementioned phases. The manifestation of a GTCS event can be characterized by an onset that involves a increased muscle tone usually accompanied with irregular and asymmetric jerking followed by tremulousness that translates into clonic activity before subsiding gradually. The frequency of the clonic jerks decreases as the event terminates and we have termed this as the subsiding behavior of an event. Based on these observations, we propose two new indexes that captures the onset and the subsiding behavior of an event; (1) tonic index (*TI*), and (2) dispersion decay index (*DDI*). Fig. 1 shows the accelerometer traces of recorded events from our dataset. The events highlights different manifestation phases, based on their clinical aetiology.

III. Method

A. Participants and Data Aquisition

Patients undergoing VEM at the video telemetry unit of the Royal Melbourne Hospital were recruited in the study. Patients were assessed based on the history and description of the seizures. Patients with a history of seizures that mimics generalized seizures or are characterized by the presence of bilateral convulsions were recruited in the study. Patients with a history of partial/complex or non-convulsive seizures were excluded from the study. Further, patients having intracranial monitoring or suffering from psychiatric disorder such that it prevents informed consent were excluded from the study. The patients were recruited for the hole duration of VEM lasting a minimum of three days.

A wireless device with an MEMS accelerometer sensor was strapped on the wrists of the recruited patients. The

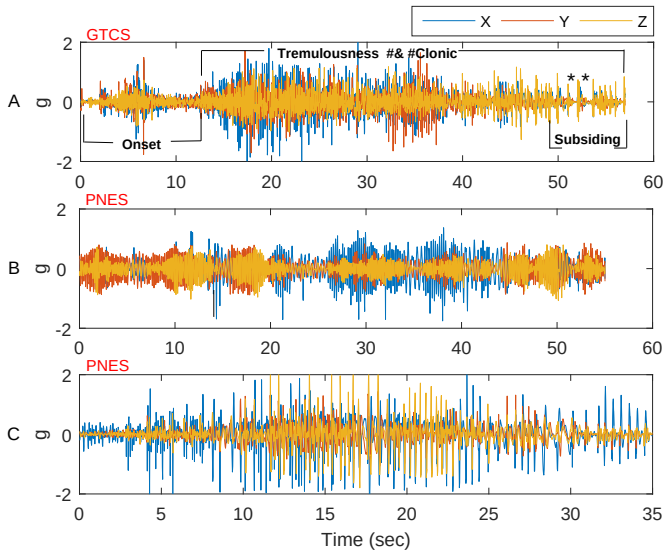

Fig. 1: Accelerometer traces of a typical: (A) GTCS event with demarcations highlighting onset, tremulousness + clonic, and subsiding behavior. The asterisk (∗) shows the silent periods during the subsiding period. (B) convulsive PNES event where the tonic and the clonic phase are not separable. The envelope of the event is continuously waxing and wanning over the course of an event. (C) A convulsive PNES event stereotypical of a clonus. Observe that the event does not have a tonic phase; it begins gradually and manifest as clonus activity.

data packets were sampled at a rate of 50Hz. Movement data recorded in three axes with a time stamp is saved on the flash memory of the device and is later extracted for offline processing. In a study spanned over $2012-2015$ a total of 79 patients were recruited in the study. Out of 79 patients, 35 (44.3%) had seizures among which 20 (25.3%) patients had convulsive seizures and 15 (18.98%) patients had non-convulsive seizures. Out of 20 patients with convulsive seizures 11 (55%) had GTCS events, 6 (30%) had PNES events, 1 had complex partial seizures (CPS), 1 had multiple types of seizures (GTCS+CPS), and 1 patients had co-morbid epilepsy (PNES+GTCS). A total of 83 events were recorded during the monitoring period, which included 39 (46.98%) GTCS from $12/79$ (15.18%) patients and 44 (53.01%) convulsive PNES events from $7/79$ (8.8%) patients.

B. Diagnosis of PNES versus GTCS

A PNES event is defined as a sporadic paroxysmal event that may involve partial or complete loss of conscious behavior coupled with a rhythmic movement of limbs (typical of a generalized seizure), in the absence of ictal electrical discharge [2]. The diagnosis of all recorded convulsive events was determined at a consensus meeting of epileptologists where a decision was made based on the clinical history, neuroscychiatric evaluation, neuroimaging studies, video-EEG and observed seizure semiology. This classification of the seizures by epileptologists is the gold standard method and is used as the ground truth. During the complete procedure epileptologists were blinded to the accelerometer traces.

C. Extraction of Temporal Variations in Limb Movement

Time stamped accelerometer traces corresponding to seizure events were used to extract the resultant accelerometer signal R ($R = sqrt(a_x^2 + a_y^2 + a_z^2)$) where, a_x, a_y, and a_z is the accelerometer data corresponding to three Cartesian axes. The resultant accelerometer data was then filtered to remove the effect of static gravity and frequencies above 25Hz. The cut-off frequency is chosen empirically based on the analysis of rhythmic artifacts as seen on EEG. The temporal variations are then extracted from the resultant accelerometer traces.

Poincaré maps can be used to extract temporal variations in time series data. Poincaré maps have been used to study time varying signals like ECG derived HRV [17]. Rhythmic and chaotic patterns in a time varying sequence can be captured using Poincaré maps [23]. Poincaré map is a geometrical representation of the time series data, obtained by plotting each sequence in a series against the following interval. An ellipse can be fitted to a Poincaré map and standard descriptors like $SD1$ and $SD2$ that represents the minor and major axis of the ellipse can be derived as shown in (1) and (2). Fig. 2 shows the standard $2-D$ Poincaré map of a time series signal at $lag = 1$ with a fitted ellipse.

$$SD1^2 = \frac{1}{\sqrt{2}} Var\big(r(n) - r(n+1)\big) \tag{1}$$

$$SD2^2 = Var\big(r(n) + r(n+1) - 2\bar{r}\big) \tag{2}$$

where, $r(n)$ denotes the time course of an event $n \in [1 \ldots N]$, $r(n+1)$ represents the sequence at $lag = 1$, and $\bar{r} = E[r(n)]$.

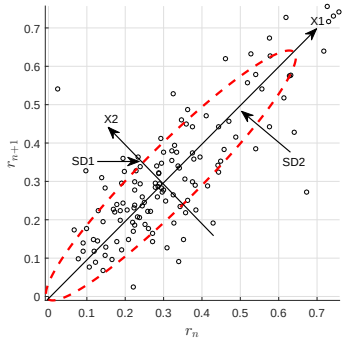

Fig. 2: A Poincaré map is a graphical representation of correlation between successive points in a non-stationary data. The Poincaré map can be visualized as a point cloud oriented along the line of identity. An example Poincaré map of resultant accelerometer time series signal; showing the fitted ellipse (dotted in red) and the standard descriptors ($SD2$, and $SD1$) as measured along the line of identity and along the line perpendicular to it.

$SD1$ and $SD2$ are shown to capture the short and long-term variations in the time-series data [17]. In addition, multiple parameters can be extracted from a Poincaré maps. Parameters like $\widehat{ratio}$ ($SD1/SD2$) and $\widehat{area}$ ($4 \times \pi \times SD1 \times SD2$) obtained

using the standard Poincaré descriptors captures the non-linear dynamics of a non-stationary time sequence [16].

The temporal variations of Poincaré descriptors can be estimated by analyzing the progression of standard Poincaré descriptors over the course of an event. However, as different events can have varied event duration, the temporal progression of the Poincaré descriptors can only be compared across events, if the duration of all events is made same on the time axis. Therefore, all the events are re-sampled using cubic splines to a fixed event duration of 60*s*. The re-sampling of the events does not change the frequency content of the signal and the temporal patterns in the signal are restored. Furthermore, GTCS events have been shown to have a mean duration of 60*s* [22], thus it is only justifiable to re-sample the events to a uniform length of 60*s*.

The resultant accelerometer signal corresponding to the re-sampled event is analyzed in time epoch's of 2.56*s* with 50% overlap resulting in a total of 45 epoch's (Fig. 3 B). Poincaré maps were obtained for every epoch resulting in a graphical representation of every sequence as a function of the previous one (Fig. 3 C, and Fig. 3 D). Descriptors capturing both linear ($\widehat{SD1}$, and $\widehat{SD2}$) and non-linear dynamics ($\widehat{ratio}$, and $\widehat{area}$) were computed from each Poincaré map which embeds the temporal information in GTCS and convulsive PNES events (Fig. 3 E, F, G, and H).

D. Protocol for Analysis of Temporal Variations

To study the onset, transition, and the subsiding period we segmented the re-sampled event (duration 60*s*) into quartiles. This allows us to study the temporal variability in Poincaré descriptors across different phases of an event. Fig. 3 I, shows the analysis protocol.

E. Quantification of temporal variability

To quantify the tonic-phase in an event we introduce a new parameter in this work, which is termed as tonic index of an event. Whereas, to capture the subsiding nature of an event we introduce another parameter that is termed as dispersion decay index. Both, the indexes are described herewith:

a) TI: The tonic index (TI) can be described as the ratio of the coefficient of variation (CoV) of the descriptor in first quartile (onset) to CoV of the descriptor over rest of the signal (transition + subsiding period). CoV is a standardized measure of variance of a probability distribution thus, giving a mean normalized measure of variance. TI can be explained as shown in (3).

$$TI_D = \frac{CoV(\{D_{k1}\})}{Cov(\{D_{k2}\})} \tag{3}$$

where, $\{D\}$ represents a discrete time series for D^{th} descriptor ($D \in \{\widehat{SD1}, \widehat{SD2}, \widehat{area}, \widehat{ratio}\}$), $1 \leq k1 \leq \lfloor \frac{N}{4} \rfloor$, $\lfloor \frac{N}{4} + 1 \rfloor \leq k2 \leq N$, and $N = 45$ is the total number of 2.56*s* windows with 50% overlap for an event with duration 60*s*.

b) DDI: The dispersion decay index (*DDI*) measures the relative change in dispersion or randomness as an event subsides. *DDI* captures the variance or randomness of an event in first three quartiles relative to the last quartile. The *DDI* can be described as shown in (4).

$$DDI_D = \frac{Var(\{D_{k1}\})}{Var(\{D_{k2}\})} \tag{4}$$

where, $\{D\}$ represents a discrete time series for D^{th} descriptor ($D \in \{\widehat{SD1}, \widehat{SD2}, \widehat{area}, \widehat{ratio}\}$), $1 \leq k1 \leq \lfloor \frac{3^*N}{4} \rfloor$, $\lfloor \frac{3^*N}{4} + 1 \rfloor \leq k2 \leq N$, and $N = 45$ is the total number of 2.56*s* windows with 50% overlap for an event with duration 60*s*.

F. Statistical Analysis

The statistical analysis includes the two sided non-parametric Mann-Whitney U test to compare the mean values of TI and *DDI* index for GTCS and convulsive PNES events. Further, analysis included the receiver operator characteristics (ROC) curve to asses the performance of the two proposed indexes (TI, and *DDI*) in classification of GTCS and PNES using Poincaré derived temporal variations.

All the statistical analysis was performed using Matlab2015b (MathWorks, Natick, MA, U.S.A.). Two-tailed Mann-Whitney U test was employed as the samples in two classes stem from two unrelated distributions with different sample sizes. The statistical significance was considered for $p \leq 0.001$ and area under the ROC curve (AUC) was used to evaluate the classification performance.

G. Blinded Review

To validate the clinical usefulness and the potential of the proposed features a blinded review was conducted by presenting the temporal evolution of extracted Poincaré descriptors to 2 board certified clinical neurologists (co-authors B.Yan, and T.J O'brien). The clinicians had to label the events either into GTCS or convulsive PNES, otherwise classify the event as non-diagnostic. During the whole exercise the clinicians were blinded to the ground truth (VEM diagnosis) and all other neurophysiologic data.

H. Statistical Machine Learning

AUC was employed to assess the classification performance of individual descriptor; however, AUC can only be used to assess the performance of a single feature vector. Thus, to evaluate the classification performance of combination of TI and *DDI* of all Poincaré descriptors, we employed linear discriminant analysis (LDA) for classification. A leave one event out cross-validation was performed where, a classification function (LDA) was trained using data from $n-1$ events ($n = 83$) and the learned classification model was then used to predict the membership of omitted event. The classification performance is reported in terms of PNES detection sensitivity, specificity, positive predictive value (PPV), negative predictive value (NPV), and the leave one out error (LOOE).

IV. Results

The temporal variations of the Poincaré derived descriptors across all GTCS and convulsive PNES events are shown in Fig. 4. The temporal variations in $\widehat{SD1}$, $\widehat{SD2}$, $\widehat{ratio}$, and

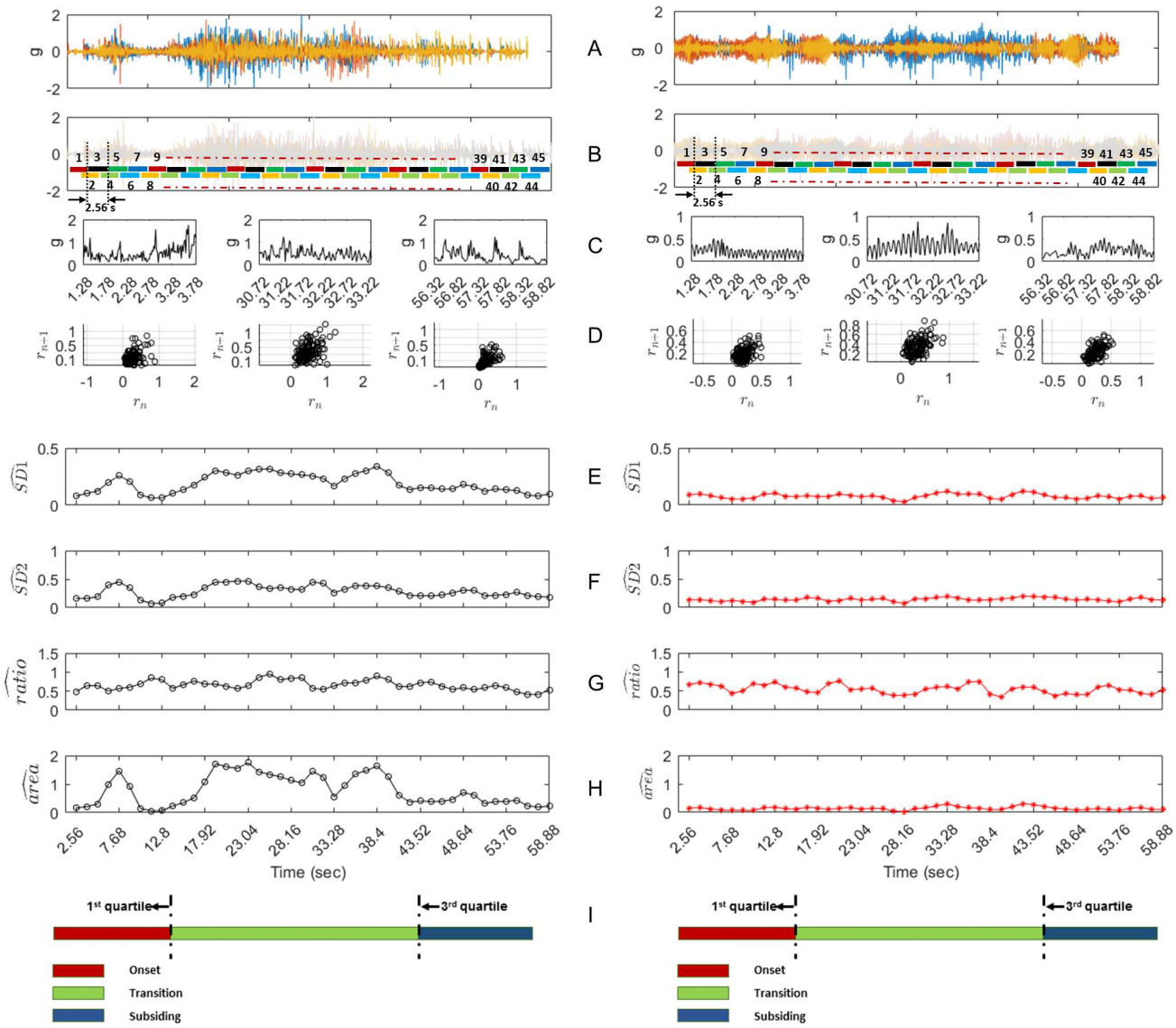

Fig. 3: Protocol for analysis of temporal variations: column one shows a GTCS and column two shows a PNES event; In each column (A) is raw signal, (B) shows the signal after re-sampling to 60*s*. The re-sampled signal is analyzed in 2.56*s* epoch's with 50% overlap, and a total of 45 epoch's are obtained by this windowing procedure. The epoch's are shown by colored blocks of 2.56*s*; (C) shows 2.56*s* accelerometer epoch's (resultant signal) during start (1.28-3.78*s*), during (30.72-33.22*s*), and at the end of an event (56.32-58.82); (D) shows the Poincaré maps corresponding to each 2.56*s* epoch; (E), (F), (G), and (H) shows temporal evolution of extracted Poincaré features in windows of 2.56*s* over the course of an event, and (I) shows the division of an event into quartiles where, the first quartile division (block in red) represents the temporal variations during onset while, the third quartile division (block in purple) represents the subsiding behavior, and the region (block in green) between first and third quartile represents the transition from onset to subsiding period.

$\widehat{area}$ show a different evolving pattern for GTCS and convulsive PNES. In contrast to GTCS, Poincaré derived temporal variations are more stable and show less variation over the course of an PNES event (Fig. 4). To capture the evolving pattern of events and to differentiate GTCS from convulsive PNES two new indexes are proposed: (1) tonic index (*TI*); and (2) dispersion decay index (*DDI*). The *TI*, and *DDI* of different Poincaré descriptors ($\widehat{SD1}$, $\widehat{SD2}$, $\widehat{ratio}$, and $\widehat{area}$) could differentiate GTCS from convulsive PNES events. A significant classification performance was found for the following descriptors: *TI* for $\widehat{SD1}$ (AUC 0.96, $p < 0.0001$), *TI* for $\widehat{SD2}$ (AUC 0.91, $p < 0.0001$), *TI* for $\widehat{area}$ (AUC 0.95, $p < 0.0001$), and *DDI* for $\widehat{ratio}$ (AUC 0.88, $p < 0.0001$).

A. Tonic Index

The *TI* of $\widehat{SD1}$ was significantly higher for GTCS (1.04-2.60; median 1.65; $p < 0.0001$) as compared to convulsive PNES (0.24-1.33; median 0.66) (Fig. 5a). The *TI* of $\widehat{SD1}$ resulted in an area under the ROC curve (AUC) of 0.96. This shows that a good class separation can be achieved using *TI*

TABLE I: Median, inter quartile range, and area under the ROC curve statistics for TI and DDI of Poincaré derived descriptors corresponding to GTCS and convulsive PNES events.

Index	GTCS (median ± iqr)	PNES (median ± iqr)	p-value	AUC
$TI_{\widehat{SD1}}$	1.65 ± 0.69	0.66 ± 0.22	5.48exp(−13)	0.96
$TI_{\widehat{SD2}}$	1.70 ± 1.16	0.80 ± 0.42	1.29exp(−10)	0.91
$TI_{\widehat{ratio}}$	1.05 ± 0.64	0.69 ± 0.29	7.00exp(−06)	0.78
$TI_{\widehat{area}}$	1.68 ± 0.99	0.81 ± 0.41	1.06exp(−12)	0.95
$DDI_{\widehat{SD1}}$	1.56 ± 1.48	1.05 ± 0.77	3.94exp(−05)	0.76
$DDI_{\widehat{SD2}}$	1.86 ± 1.26	0.94 ± 0.50	2.67exp(−06)	0.80
$DDI_{\widehat{ratio}}$	1.79 ± 0.70	0.92 ± 0.34	2.09exp(−09)	0.88
$DDI_{\widehat{area}}$	1.64 ± 1.57	0.98 ± 0.89	4.21exp(−04)	0.72

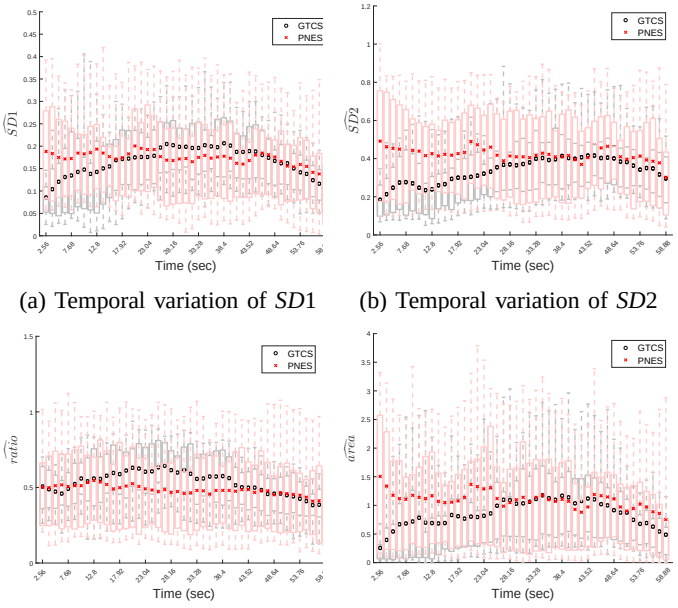

(a) Temporal variation of $SD1$ (b) Temporal variation of $SD2$

(c) Temporal variation of ratio (d) Temporal variation of area

Fig. 4: The temporal variations in Poincaré descriptors shown for every 2.56s epoch represented as box and whisker plots for (a) $\widehat{SD1}$, (b) $\widehat{SD2}$, (c) $\widehat{ratio}$, and (d) $\widehat{area}$. The ∘ in black represents the mean in every 2.56s epoch for GTCS and × in red for convulsive PNES. Please note that the temporal variation of descriptors for a convulsive PNES event shows less variability over the course of an event in comparison to GTCS.

of $\widehat{SD1}$. Similarly the TI of $\widehat{SD2}$ was significantly higher for GTCS (0.83-3.64; median 1.70; $p < 0.0001$) in comparison to convulsive PNES (0.21-1.43; median 0.80) (Fig. 5a). An AUC value of 0.91 could be achieved using TI of $\widehat{SD2}$. Further, the TI of $\widehat{area}$ was also significantly higher for GTCS (1.04-2.99; median 1.68; $p < 0.0001$) in comparison to convulsive PNES (0.27-1.34; median 0.81) (Fig. 5a) and showed an AUC value of 0.95. In contrast, the TI of $\widehat{ratio}$ was found to have a much lower AUC value of 0.78 while, having a significant difference between GTCS (0.46-2.40; median 1.05; $p < 0.0001$) and convulsive PNES (0.29-1.29; median 0.69) (Fig. 5a). It can be seen that the TI performs well for all the descriptors except $\widehat{ratio}$, and the TI of $\widehat{SD1}$ showed best class separation between GTCS and convulsive PNES with an AUC value of 0.96 (Table I).

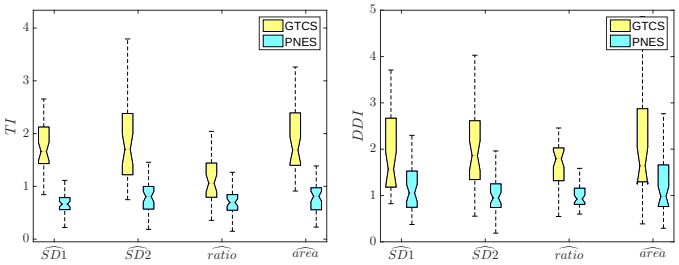

(a) TI of descriptors (b) DDI of descriptors

Fig. 5: (a) The TI, and (b) DDI for descriptors $\widehat{SD1}$, $\widehat{SD2}$, $\widehat{ratio}$, and $\widehat{area}$ shown as box and whisker plots for GTCS and convulsive PNES events.

B. Dispersion Decay Index

The DDI of $\widehat{SD1}$ was significantly different for GTCS (0.87-4.57; median 1.56; $p < 0.001$) and convulsive PNES (0.46-2.57; median 1.05) (Fig. 5b) events with an area under the ROC curve of 0.76. Similarly, the DDI of $\widehat{SD2}$ was significantly higher for GTCS (0.67-3.23; median 1.86; $p < 0.0001$) in comparison to convulsive PNES (0.41-2.90; median 0.94) (Fig. 5b). However, the area under the ROC curve for DDI of $\widehat{SD2}$ (AUC 0.80) was slightly higher than DDI of $\widehat{SD1}$ (AUC 0.76). Similarly, the difference in DDI of $\widehat{area}$ was also statistically significant for GTCS (0.53-7.22; median 1.64; $p < 0.001$) and convulsive PNES (0.33-3.22; median 0.98) however, a considerable class overlap was seen using DDI of $\widehat{area}$ (AUC 0.72) (Fig. 5b). In contrast, the DDI of $\widehat{ratio}$ showed a better class separation (AUC 0.88). The DDI of $\widehat{ratio}$ was significantly higher for GTCS (0.92-2.87; median 1.79; $p < 0.0001$) in comparison to convulsive PNES (0.64-1.53; median 0.92) (Fig. 5b). Thus, it can be seen that the DDI of $\widehat{ratio}$ shows the highest class separation between GTCS and convulsive PNES, which suggests that ratio is the most efficient Poincaré descriptor to capture dispersion or randomness in movement of limbs as an event subsides. Table I shows the statistical measures for TI and DDI corresponding to the derived measures of temporal variations in GTCS and convulsive PNES events.

C. Combination of TI and DDI

Both TI, and DDI were significantly higher for GTCS events (Table I, and Fig. 5). Using TI, and DDI of all descriptors (total 8 features as shown in Table I) a classification model

TABLE II: The diagnostic performance of the proposed approach based on the blinded analysis of Poincaré descriptors; and based on a classifier build using a combination of TI and DDI of all descriptors.

Blinded Review							Automation – Combination of TI & DDI						
	PNES		GTCS		VEM			PNES		GTCS		VEM	
PNES	26		11		44		PNES	42		2		44	
GTCS	5		33		39		GTCS	3		36		39	
Diagnosis	31		44				Diagnosis	45		38			
Sens*	Spec*	PPV*	NPV*	LOOE*	Non-diagnsotic		Sens*	Spec*	PPV*	NPV*	LOOE*	Non-diagnostic	
70.27%	86.84%	83.87%	75.00%	N/A	8		95.45%	92.30%	93.33%	94.73%	6.02%	N/A	

* Statistical measures of performance; Sens: sensitivity ($\frac{TP}{TP+FN}$); Spec: specificity ($\frac{TN}{TN+FP}$); PPV: positive predictive value ($\frac{TP}{TP+FP}$); NPV: negative predictive value ($\frac{TN}{TN+FN}$); LOOE: leave one out error.

was build using linear discriminant analysis. The machine learning model correctly classified seizure like events as PNES in 42 (sensitivity: 95.45%) of 44 PNES events and being as GTCS in 36 (specificity: 92.30%) of 39 GTCS events (Table II). The PPV, NPV, and LOOE were 93.33%, 94.73%, and 6.02%, respectively.

D. Blinded Review

Based on the temporal dynamics of GTCS and convulsive PNES the following criterion were defined for differentiation of GTCS and PNES: the Poincaré derived temporal variations in $SD1$, $SD2$, and *area* shows a gradual onset (tonic-phase) followed by a continuously evolving nature representing the clonic phase. In contrast, the temporal dynamics of Poincaré derived descriptors were rather stable over the course of a convulsive PNES event. Two of the co-authors (B.Y, and T.J.O) were presented the Poincaré derived temporal variations for GTCS and PNES (Fig. 3 E, F, G, and H) events in random sequence while, being blinded to all other neurophysiologic data. The blinded analysis correctly classified 26 of 44 events as PNES (sensitivity: 70.27%) and 33 of 39 as GTCS (specificity: 86.84%), with 8 of 83 events classified as non-diagnostic. The non-diagnostic events included the events that neither showed a continuously evolving nature, nor a stable manifestation.

V. Discussions

Seizures are heterogeneous in their manifestation and show intra- and inter- patient variability. There is awareness that no particular clinical feature can distinguish GTCS and PNES in all patients. In this work, we present an approach based on quantifying the rhythmic limb movement during GTCS and convulsive PNES captured using a wrist-worn wireless accelerometer sensor. We employed Poincaré analysis to find the hidden correlation patterns between non-stationary time varying accelerometer signals. The temporal variations in Poincaré descriptors ($\widehat{SD1}$, $\widehat{SD2}$, $\widehat{area}$, and $\widehat{ratio}$) extracted over the course of an GTCS and convulsive PNES event showed variation across the two groups (Fig. 4). However, the variability was observed at group level and to distinguish events at individual level we need to capture variations that are specific to a particular phase of an event. To quantify this temporal variation, we presented two new indexes: (1) tonic index (TI); and (2) dispersion decay index (DDI).

a) The Tonic Index: The onset of a GTCS event has a defined organic pathway and can be captured by a movement recording sensor [24]. To quantify the onset of an event we introduce a new parameter in this work, which is termed as the tonic index of an event. TI captures the mean normalized variability during onset relative to rest of the signal. Therefore, if an event does not have a distinct tonic phase it will have a low TI value and vice versa. An underlying assumption is that, the onset of an event will be captured by the first quarter (after resampling the event to 60s) of an event.

b) The Dispersion Decay Index: Another, differentiating factor between GTCS and convulsive PNES can be the pattern in which the two events terminates. In contrast to PNES, GTCS events have a gradual subsiding nature that may include silent periods as shown by ($*$) in Fig. 1. Whereas, PNES events are relatively stable over time and manifest in periodic and repetitive movements that rapidly decreases in amplitude as event terminates. The motor manifestation of GTCS events has a comparatively higher variability presumed to have resulted from the excessive or hyper-synchronous electrical discharge from neurons. The clonic-phase of a GTCS event involves high frequency jerk like movements that subsides gradually as the event terminates. This brings us to another parameter that captures the gradual decaying or subsiding nature of an event and is termed as dispersion decay index (DDI). Therefore, if an event involves clonic jerks that subsides gradually the event will have a high DDI value. Again, an underlying assumption while calculating DDI is that, the last quarter (after resampling the event to 60s) represents the subsiding behavior of an event.

A. Performance Of The Proposed Approach

Two indexes differentiated between GTCS and convulsive PNES: the tonic index (TI), and dispersion decay index (DDI). TI quantifies the variability in onset relative to rest of the event. The TI of all descriptors showed a significant class separation between GTCS and convulsive PNES (Table I). $TI_{\widehat{SD1}}$, and $TI_{\widehat{SD2}}$ resulted in an AUC of 0.96, and 0.91, respectively (Table I). $SD1$ and $SD2$ captures the short and long-term changes in a time sequence [17]. The onset of a GTCS event involves increased muscle tone represented by stiffening movement of limbs manifesting as long-term variations and resulting to a higher $SD2$, and a lower $SD1$. Whereas, as the muscle tone decreases and the high frequency clonic jerking begins the magnitude of $SD1$ becomes higher while, $SD2$ decreases in magnitude. In contrast, both $SD1$ and $SD2$ were rather stable or had lesser variability over the course

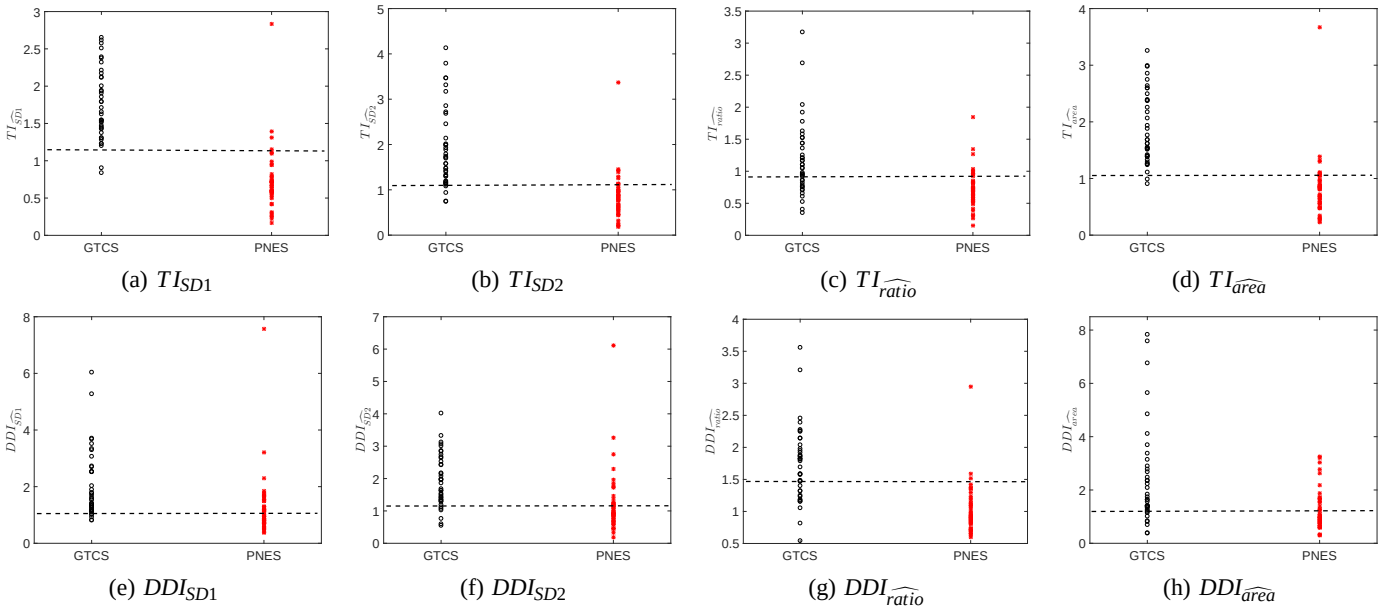

(a) TI_{SD1} (b) TI_{SD2} (c) $TI_{\widehat{ratio}}$ (d) $TI_{\widehat{area}}$

(e) DDI_{SD1} (f) DDI_{SD2} (g) $DDI_{\widehat{ratio}}$ (h) $DDI_{\widehat{area}}$

Fig. 6: TI (a)-(d), and DDI (e)-(h) of descriptors $\widehat{SD1}$, $\widehat{SD2}$, $\widehat{ratio}$, $\widehat{area}$ for GTCS and convulsive PNES events ($n = 89$). The dotted line represents the linear threshold corresponding to the optimal operating point of the ROC curve.

of a convulsive PNES event (Fig. 4). Therefore, TI of $SD1$ and $SD2$ showed a high class separation between GTCS and convulsive PNES. On the other hand, $\widehat{ratio}$ and $\widehat{area}$ are proxy measures that are derived from standard descriptors $SD1$ and $SD2$. $TI_{\widehat{ratio}}$, and $TI_{\widehat{area}}$ resulted in an AUC of 0.78, and 0.95, respectively. Ratio is a measure of randomness or dispersion of a time sequence. The onset of events often involves irregular and asymmetric jerking movements. Thus, onset of both GTCS and convulsive PNES events have a lower randomness in contrast to clonus activity. Therefore in comparison to other descriptors, TI of ratio ($TI_{\widehat{ratio}}$) leads to a lower AUC (0.78) (Table I, and Fig. 5a).

While the temporal variations during onset are captured by TI, the subsiding pattern of an event is captured by DDI. The DDI of all the descriptors showed a significant class separation between GTCS and convulsive PNES (TABLE I). The highest AUC (0.88) was obtained for $DDI_{\widehat{ratio}}$. DDI measures the variance in two-third of the signal relative to the last quartile. The high frequency clonic jerks in GTCS can be characterized by an increased dispersion or a chaotic manifestation of the accelerometer traces. The frequency of the jerks reduces as the event terminates which results in a lower dispersion in the last quartile. Therefore, DDI of ratio ($DDI_{\widehat{ratio}}$) results in the highest AUC (Table I, and Fig. 5b).

Among TI and DDI of all descriptors, $TI_{\widehat{SD1}}$ and $TI_{\widehat{SD2}}$ showed a higher class separation (Fig. 5, and Table I). The better performance of $TI_{\widehat{SD1}}$ and $TI_{\widehat{SD2}}$, can be attributed to the higher temporal variations in GTCS than convulsive PNES (Fig. 4). These findings indicate that, convulsive PNES events have a characteristic non-evolving pattern on the time-scale over the course of an event (Fig. 3 E, F, G, and H). Whereas, GTCS events have distinct phases (tonic and clonic) and thus, show a continuously evolving pattern on the time scale. The findings are in agreement with Vinton *et al.* [25], who showed that convulsive PNES events displays a characteristic pattern with a stable, non-evolving frequency footprint.

The TI and DDI of the Poincaré descriptors showed significant difference between GTCS and convulsive PNES at group level (TABLE I) however, some overlap existed among events at the individual level (Fig. 5). Fig. 6a shows the box plot for $TI_{\widehat{SD1}}$; the group medians for GTCS and convulsive PNES differed significantly (GTCS 1.65; PNES 0.66; $p < 0.001$). The linear threshold ($TI = 1.20$) corresponds to the optimal operating point of the ROC curve. The linear threshold could distinguish 37 (94.87%) of 39 GTCS, and 40 (90.90%) of 44 convulsive PNES. However, the threshold and the performance varied across descriptors for both the TI, and DDI (Fig. 6). Therefore, a statistical learning approach was utilized to study the classification performance of the combination of TI and DDI of all descriptors (a total of 8 features). A classifier (LDA) was trained and validated in a leave-one-event-out method. The LDA classifier achieved a PNES detection sensitivity of 95.45%, specificity of 92.30%, PPV of 93.33%, and a LOOE of 6.02% (Table II). Two PNES and three GTCS events were misclassified by the automated approach. The two PNES events corresponded to patient P_{15} **(refer to Table I, supplementary material)**. Both, the events involved unilateral and rhythmic tapping of the hands, that manifested in short bursts of repetitive motor activity. Therefore, temporal variations in $SD1$ and $SD2$ showed continuously evolving nature thus, leading to misclassification of the events. Interestingly, the $TI_{\widehat{ratio}}$ alone correctly differentiated both the PNES events. $\widehat{ratio}$ is a non-linear descriptor that takes into account the variation in both $SD1$ and $SD2$. $\widehat{ratio}$ was stable over the course of the events, and showed a non-evolving pattern. The $TI_{\widehat{ratio}}$ was significantly lower for both the PNES events in comparison to all GTCS events (GTCS: 1.059, misclassified PNES events: 0.5344, $p = 0.0492$). Therefore, it would be

interesting to investigate other non-linear descriptors like complex correlation measure (CCM) [26], in differentiation of GTCS and convulsive PNES. The 3 GTCS events that were misclassified by the automated approach corresponded to patient P_{11} (1 event each from the left and the right hand device corresponding to a single GTCS event), and P_{12} (event recorded from the left hand device) **(refer to Table I in supplementary material)**. The misclassified event corresponding to P_{11} had a clonic phase preceding the tonic phase thus, the event was clonic-tonic rater than tonic-clonic in manifestation. Intuitively, TI and DDI are designed to capture and differentiate the tonic-clonic manifestation of GTCS events therefore, both TI and DDI of descriptors misclassified the clonic-tonic event of P_{11}. Whereas, the GTCS event of P_{12} did not have an evident tonic-phase and the event was more clonic. As the event only involved clonus activity, the Poincaré derived temporal variations did not have the typical evolving nature associated with GTCS events. Interestingly, the event was labeled as non-diagnostic during the blinded review by expert epileptologists. Based on the above results it would be safe to assume that, the two proposed indexes (TI, and DDI) are efficient in differentiating GTCS from convulsive PNES; unless, an event has a manifestation that differs from the clinically defined motor symptomatology.

Further, the statistical classifier results in a diagnostic accuracy that was superior to blinded review of temporal variations in Poincaré descriptors by expert epileptologists (Table II). The 7 (87.5%) of 8 events (7 PNES and 1 GTCS) labeled as non-diagnostic by the epileptologists belonged to a single patient **(P_{17}; refer to Table I in supplementary material)**. The automated approach correctly identified all the 7 PNES events. Therefore, the automated approach based on TI and DDI shows the potential to be used as tool to assist epileptologists, in differentiation of GTCS and convulsive PNES.

The current gold standard for establishing diagnosis of convulsive PNES is as done in comprehensive Epilepsy program meetings where, information regarding neuropsychiatric evaluation, radiology, clinical history, and video recording are analyzed. The proposed method will be a value addition to the tools of epileptologists, as the two proposed indexes (TI and DDI) gives a non-linear projection of the $3-D$ rhythmic limb movement into a numerical score. TI and DDI can be utilized to distinguish GTCS and convulsive PNES either based on: (1) the thresholds derived from the optimal operating point of the ROC curve (Fig. 6), or (2) based on the predictions made using a trained statistical classifier (Table II).

B. Comparisons With Existing Studies

Wearable non-EEG based devices for differentiation of GTCS and PNES are seldom discussed. Few research groups have investigated the use of ECG derived HRV and sEMG sensor in differential diagnosis of PNES [20] [19]. ECG derived HRV showed a PNES detection sensitivity of 88% [20]. However, ECG based system may not be suitable for ambulatory setting, as the heart rate changes may vary with the vigilance state of the person. Beniczky *et al.* [19] proposed an ambulatory system based on sEMG measurements recorded from deltoid muscles. They showed that the HF/LF ratio (HF: high-frequency 64-256 Hz; LF: low-frequency 2-8 Hz) and RMS of the sEMG signal could differentiate all GTCS from convulsive PNES (sensitivity 100%). However, the proposed approach has several advantages over an sEMG based system as: continuous use of sEMG electrodes can be uncomfortable and has a potential for detachment [27]. In contrast, the proposed system is an electrode less system thus being more comfortable and less encumbering to the patient [21]. In addition, the proposed approach is based on a time-domain analysis which is computationally efficient and gives an opportunity for real-time analysis [18].

Furthermore, the proposed approach showed a better performance in distinguishing GTCS and convulsive PNES (Table I) in comparison to the frequency-domain approach presented earlier (AUC 0.78) [15]. In contrast to our earlier work [15], in this study the data was acquired using a wireless accelerometer. Therefore, due to the nature of the data pre-processing the collected data is sparse thus, approach based on FFT is not robust. For further details on data collection and pre-processing please refer to our previous work [13].

C. Clinical Utility Of The Proposed Approach

Despite of the observed differences in pathophysiology of GTCS and convulsive PNES, a significantly higher proportion of patients with PNES are misdiagnosed. The misdiagnosis of convulsive PNES detracts from the correct treatment and exposes the patient to side-effects of AED's. In addition, misdiagnosis delays the correct treatment of the underlying psychology and enforces financial, social, and emotional consequences on the patient. It has been found that a significantly higher number of patients with PNES are initially misdiagnosed as epileptic [28]. This misdiagnosis does not have an impact only on the patient, however it is also associated with the increased financial burden on the healthcare system [7] [8]. Further, PNES patients may also have a co-existing epilepsy which might escalate the delay in correct diagnosis [1]. This delayed diagnosis of PNES, indicates possible gaps in the current diagnostic procedures and a need to intervene with a more object method to assist clinicans, neurlogoists and epileptologists in diagnosis. A timely diagnosis of PNES can greatly improve the treatment outcome for patients [11]. Based, on the encouraging results of the proposed study it can be said that the proposed accelerometer based system can overcome the limitations of the current diagnostic procedures and aid in better prognosis and treatment of patient with PNES.

ACKNOWLEDGMENT

We are grateful to all the patients who agreed to be a part of the study and extend gratitude to the staff and honors students of Melbourne Brain Center for aiding in data collection. Disclosure: None of the authors have any conflict of interest to be disclosed.

REFERENCES

[1] S. G. Jones *et al.*, "Clinical characteristics and outcome in patients with psychogenic nonepileptic seizures," *Psychosomatic medicine*, vol. 72, no. 5, pp. 487–497, 2010.

[2] M. Reuber, "Psychogenic nonepileptic seizures: answers and questions," *Epilepsy & Behavior*, vol. 12, no. 4, pp. 622–635, 2008.

[3] W. C. LaFrance and O. Devinsky, "Treatment of nonepileptic seizures," *Epilepsy & Behavior*, vol. 3, no. 5, pp. 19–23, 2002.

[4] W. C. LaFrance *et al.*, "Minimum requirements for the diagnosis of psychogenic nonepileptic seizures: a staged approach," *Epilepsia*, vol. 54, no. 11, pp. 2005–2018, 2013.

[5] P. E. Smith, "Epilepsy: mimics, borderland and chameleons," *Practical neurology*, vol. 12, no. 5, pp. 299–307, 2012.

[6] O. Devinsky, D. Gazzola, and W. C. LaFrance, "Differentiating between nonepileptic and epileptic seizures," *Nature Reviews Neurology*, vol. 7, no. 4, pp. 210–220, 2011.

[7] M. Reuber *et al.*, "Diagnostic delay in psychogenic nonepileptic seizures," *Neurology*, vol. 58, no. 3, pp. 493–495, 2002.

[8] ——, "Failure to recognize psychogenic nonepileptic seizures may cause death," *Neurology*, vol. 62, no. 5, pp. 834–835, 2004.

[9] ——, "Somatization, dissociation and general psychopathology in patients with psychogenic non-epileptic seizures," *Epilepsy research*, vol. 57, no. 2, pp. 159–167, 2003.

[10] J. Alving and S. Beniczky, "Diagnostic usefulness and duration of the inpatient long-term video-eeg monitoring: findings in patients extensively investigated before the monitoring," *Seizure*, vol. 18, no. 7, pp. 470–473, 2009.

[11] M. Reuber *et al.*, "Outcome in psychogenic nonepileptic seizures: 1 to 10-year follow-up in 164 patients," *Annals of neurology*, vol. 53, no. 3, pp. 305–311, 2003.

[12] J. van Andel *et al.*, "Non-eeg based ambulatory seizure detection designed for home use: what is available and how will it influence epilepsy care?" *Epilepsy & Behavior*, vol. 57, pp. 82–89, 2016.

[13] J. Gubbi *et al.*, "Automatic detection and classification of convulsive psychogenic non-epileptic seizures using a wearable device," *IEEE Journal of Biomedical and Health Informatics*, vol. PP, no. 99, Jun 2015.

[14] S. Kusmakar *et al.*, "Automated detection of convulsive seizures using a single wrist-worn accelerometer device," IEEE Transactions on Biomedical Engineering, Submitted.

[15] J. Bayly *et al.*, "Time-frequency mapping of the rhythmic limb movements distinguishes convulsive epileptic from psychogenic nonepileptic seizures," *Epilepsia*, vol. 54, no. 8, pp. 1402–1408, 2013.

[16] M. Brennan, M. Palaniswami, and P. Kamen, "Do existing measures of poincare plot geometry reflect nonlinear features of heart rate variability?" *IEEE transactions on biomedical engineering*, vol. 48, no. 11, pp. 1342–1347, 2001.

[17] A. H. Khandoker, C. Karmakar, and M. Brennan, *Poincaré plot methods for heart rate variability analysis*. Springer.

[18] L. Logesparan, A. J. Casson, and E. Rodriguez-Villegas, "Optimal features for online seizure detection," *Medical & biological engineering & computing*, vol. 50, no. 7, pp. 659–669, 2012.

[19] S. Beniczky *et al.*, "Quantitative analysis of surface electromyography during epileptic and nonepileptic convulsive seizures," *Epilepsia*, vol. 55, no. 7, pp. 1128–1134, 2014.

[20] A. Ponnusamy, J. L. Marques, and M. Reuber, "Comparison of heart rate variability parameters during complex partial seizures and psychogenic nonepileptic seizures," *Epilepsia*, vol. 53, no. 8, pp. 1314–1321, 2012.

[21] A. Schulze-Bonhage *et al.*, "Views of patients with epilepsy on seizure prediction devices," *Epilepsy & behavior*, vol. 18, no. 4, pp. 388–396, 2010.

[22] W. Theodore *et al.*, "The secondarily generalized tonic-clonic seizure a videotape analysis," *Neurology*, vol. 44, no. 8, pp. 1403–1403, 1994.

[23] C. A. Del Negro *et al.*, "Periodicity, mixed-mode oscillations, and quasiperiodicityin a rhythm-generating neural network," *Biophysical Journal*, vol. 82, no. 1, pp. 206–214, 2002.

[24] E. Schulc *et al.*, "Measurement and quantification of generalized tonic–clonic seizures in epilepsy patients by means of accelerometryan explorative study," *Epilepsy research*, vol. 95, no. 1, pp. 173–183, 2011.

[25] A. Vinton *et al.*, "convulsive nonepileptic seizures have a characteristic pattern of rhythmic artifact distinguishing them from convulsive epileptic seizures," *Epilepsia*, vol. 45, no. 11, pp. 1344–1350, 2004.

[26] C. K. Karmakar *et al.*, "Complex correlation measure: a novel descriptor for poincaré plot," *Biomed. engg. online*, vol. 8, no. 1, p. 1, 2009.

[27] A. Ulate-Campos *et al.*, "Automated seizure detection systems and their effectiveness for each type of seizure," *Seizure*, vol. 40, pp. 88–101, 2016.

[28] S. R. Benbadis and W. A. Hauser, "An estimate of the prevalence of psychogenic non-epileptic seizures," *Seizure*, vol. 9, no. 4, pp. 280–281, 2000.